

Madalin-Stefan Radu, Cristian Sarpe, Elena Ramela Ciobotea, Bastian Zielinski, Radu Constantinescu, Thomas Baumert and Camilo Florian*

Temporal airy pulses efficiency in thin glass dicing

<https://doi.org/10.1515/zpch-2024-0911>

Received May 31, 2024; accepted October 15, 2024; published online November 14, 2024

Abstract: Ultrashort pulse laser sources are useful tools for micro- and nano-processing large band gap dielectric materials. One of the biggest advantages of these pulses is the possibility to reach high intensity peaks that promote absorption even in materials transparent to the laser wavelength. In addition, if the pulse temporal distribution is modified, energy absorption enables the ablation of small diameter holes with large depths. In this work, we present preliminary results that implement three types of pulses as precursors for glass dicing: Bandwidth-limited (30 fs at 785 nm), positively, and negatively dispersed Temporal Airy Pulses (TAP). The material of choice was 170 μm thick soda-lime glass, inscribed at 1 kHz repetition rate in tight (50 \times objective) and loose (20 \times objective) focusing conditions for different laser energies and scanning speeds. After laser processing, the glass was diced by mechanical stress, with a home built four-point bending stage. We analyzed the quality of the scribed lines at the surface and in cross-section after breaking, as well as the necessary breaking force for all three types of laser pulses. We report that

***Corresponding author: Camilo Florian**, Institute of Materials Engineering, University of Kassel, Moenchebergstr. 7, 34125 Kassel, Germany; and Institute of Physics and CINSaT, University of Kassel, Heinrich-Plett-Str. 40, 34132 Kassel, Germany, E-mail: camilo.florian@uni-kassel.de. <https://orcid.org/0000-0001-5632-0562>

Madalin-Stefan Radu and Radu Constantinescu, Department of Physics, Faculty of Sciences, University of Craiova, Str. Alexandru Ioan Cuza 13, 200585 Craiova, Romania. <https://orcid.org/0000-0002-3482-7394> (M.-S. Radu)

Cristian Sarpe, Department of Physics, Faculty of Sciences, University of Craiova, Str. Alexandru Ioan Cuza 13, 200585 Craiova, Romania; and Institute of Physics and CINSaT, University of Kassel, Heinrich-Plett-Str. 40, 34132 Kassel, Germany. <https://orcid.org/0000-0001-8978-7564>

Elena Ramela Ciobotea and Thomas Baumert, Institute of Physics and CINSaT, University of Kassel, Heinrich-Plett-Str. 40, 34132 Kassel, Germany. <https://orcid.org/0000-0001-6300-0161> (E.R. Ciobotea). <https://orcid.org/0000-0003-1760-7493> (T. Baumert)

Bastian Zielinski, Institute of Physics and CINSaT, University of Kassel, Heinrich-Plett-Str. 40, 34132 Kassel, Germany; and Institute of Materials Engineering, University of Kassel, Moenchebergstr. 7, 34125 Kassel, Germany. <https://orcid.org/0000-0001-5272-3540>

positive TAP produced a neat, flat-cut edge on the glass samples compared with the other implemented pulses.

Keywords: glass dicing; ultrashort pulse laser; high aspect ratio structures; laser processing; temporal pulse shaping; thin glass

1 Introduction

Materials with high hardness and low brittleness have an increasingly wide range of applications in high-end technologies. Silicon and type III-V compound semiconductors are essential to the microelectronics and optoelectronics industries. For many of these devices (e.g. power LEDs or semiconductor diodes), sapphire is used as a substrate in the epitaxial growth process.^{1,2} Soda-lime glass became the equivalent of commercial glass or flat glass due to its ease of manufacture, low cost, tough surface and recyclability,^{3–5} resulting in a notorious wide range of applications (windows, food containers, bottles, etc.). Precise cutting of the large wafers on which these components are grown is a process that determines production efficiency by reducing flawed pieces and subsequent chip quality. The earliest wafer separation techniques were two-step processes, consisting of surface scribing with diamond tips, followed by cutting. After this, diamond saw blade cutting techniques became an industry standard, used in automatic machines.⁶ In recent decades, there has been a massive tendency in the industry to reduce wafer thickness from hundreds of microns to 50–75 μm to increase the miniaturization and functionalization of the microchips.⁷ Slicing a thin wafer into microdevices by mechanical methods has many drawbacks, being a slow process with a low yield. In addition, a large kerf is produced (typically between 100 and 200 μm), and the surface quality after sawing is not acceptable for optoelectronic devices.² Laser techniques for wafer separation are based on light–matter interaction, are non-contact and precise, and overcome many of the disadvantages of diamond saw cutting. Laser-cutting technology has been used in industry for decades to cut various materials such as metals,⁸ wood,⁹ stone,¹⁰ and plastic.¹¹ Laser glass cutting is a tougher task as it can lead to breaking or shattering the glass piece. The leading technique is the use of Bessel beams,^{12,13} especially for thick glass-cutting applications. In industry, both long-pulse (nanosecond lasers) and ultrashort-pulse lasers, with pulse durations of hundreds of femtoseconds and below, are used. An advantage of the latter – having extremely high peak powers and relatively low energy – is that they can interact with the transparent dielectrics via non-linear effects, allowing material processing with minimal heat-affected zone. In previous studies,^{1,14} we have shown that temporal modulation of femtosecond pulses allows obtaining ablation structures in fused silica with diameters ranging

hundreds of nm, an order of magnitude below the limit imposed by classical optics. These structures extend over several microns deep into the material, even in the single laser-pulse processing mode. The explanation for these structures was given by how Airy time-modulated pulses control multiphoton and avalanche ionization in dielectrics, allowing the creation of a high free electron density deep in the material^{15–17} as a first step of the ablation process. Different types of glass, or hardened glass, are widely used in the flat panel display industry and the desired shape and edge quality of these pieces can only be achieved by precise and clean-cutting techniques.¹⁸ In the present study, we examine how these time-modulated pulses can be used to write ablation lines on the surface of thin soda-lime glass samples as a precursor in the dicing process. Additionally, due to its direct significance in precision glass cutting, we consider that this method could also be used successfully on sapphire or semiconductor wafers considering the similarities in the ablation process. Our experiments used laser glass dicing in a two-step process, structure modification using ultrashort laser pulses¹⁹ followed by mechanical stress.²⁰

2 Experimental setup

2.1 Laser processing

Material processing on the glass samples was performed using an amplified Ti:Sapphire based laser system (Femtolasers Femtopower-Pro), with pulse duration of 30 fs (FWHM) at 785 nm fundamental wavelength operating in 1 kHz regime on a microscope platform, as described in¹⁵. Before entering the microscope platform, the pulses were sent through an in-house designed high accuracy pulse shaper^{21,22} used both to compensate for the residual phase introduced by the optical elements in the beam path – ensuring Bandwidth-limited (BWL) pulses - and to temporally modulate the pulses using Third Order Dispersion (TOD) phases, as described in^{1,15} and shown schematically in Figure 1. A half-wave retarder and a linear polarizer placed in front of the liquid crystal modulator were used to adjust the energy of the pulses. During the processing of the sample surface, the time sequences of the applied pulses were controlled by a homemade trigger device for the Pockels cell of the amplifier.

When processing dielectrics with ultrashort laser pulses presenting a large spectral width, the dispersion introduced by optical elements plays an important role in both the threshold energies and the quality of the finished product.²³ BWL pulses are also needed as a reference when different temporal shapes of the pulses are used, especially in the case of multi-photon absorption where the processing is highly

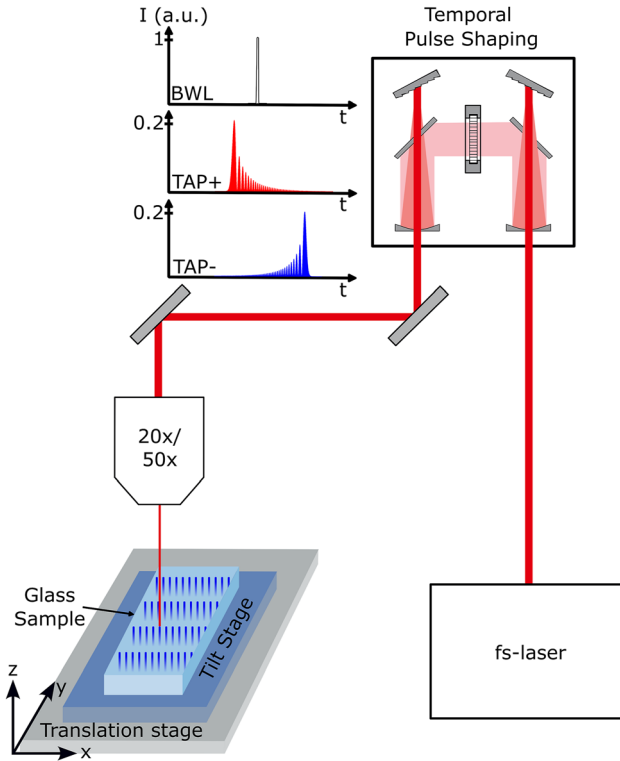


Figure 1: Experimental setup scheme.

sensitive to the intensity of the laser pulse and the BWL pulses have the highest possible peak intensity. The residual phase was compensated using a two-photon photodiode (Hamamatsu G1116) placed right in the interaction zone while trying to maximize the signal value through iterative scans of the Group Delay Dispersion (GDD) and Third-Order Dispersion parameters applied to the liquid crystal modulator. The GDD and TOD values for which the best two-photon photodiode signal was obtained were superimposed on the phases used for temporal modulation of the ultrashort pulses after the pulses passed through all optical elements (after the objective, before the focus point).

Two microscope objectives were used for this experiment, a Mitutoyo M Plan Apo SL 20 \times , 20 mm working distance, 0.42 Numerical Aperture, and a Zeiss LD Epiplan 50 \times , 7 mm working distance, 0.5 Numerical Aperture. The objectives were chosen to have irradiation conditions in which high-aspect ratio ablation structures can be obtained.^{15,24}

In a proof of principle study for the described experiments, we chose to work on thin commercial soda-lime glass slides Thorlabs Precision Glass Cover Slips, Schott D 263[®] M Glass (24 mm × 50 mm) with a thickness of $170 \pm 5 \mu\text{m}$.

The samples were placed under the microscope objective on a tilt table mounted on an XYZ translation stage controlled by stepper motors (PI miCos). The lines were written in the x-direction (parallel to the beam polarization direction under the objectives) using the native laser repetition frequency of 1 kHz, with different scanning speeds and different pulse energy. As the inscribed lines are long, across the width of the sample (24 mm) and the Rayleigh length of the lenses used is in the micrometer range, special care was taken during the measurements to align the samples so that they were as close as possible to the focal plane of the lenses throughout the processing line. Additional alignment was performed in a confocal system based on the reflection of a HeNe laser (not shown in the scheme) on the surface of the slides. It should be mentioned that no closed-loop autofocus system was used, and the native deviations from flatness ($<5 \mu\text{m}$ over 24 mm)²⁵ can influence the positioning in the focal plane of the objective. During the inscription of the laser lines on the sample surface, the interaction zone was continuously monitored using a visualization camera connected to the microscope system allowing real-time inspection and monitoring of overall progress.

Four lines, 8 mm apart, were inscribed on each slide under identical working conditions. The scribed lines were produced with different laser pulse energies at a constant writing speed, and with different writing speeds with a constant laser pulse energy. Three different laser pulse shapes were used once for each laser pulse energy and writing speed: Bandwidth-limited (BWL) pulses, positively dispersed Temporal Airy Pulses (TAP+) with a TOD of $+600.000 \text{ fs}^3$ (for which the most intense pulse in the sequence (see inset in Figure 1) propagates first and the less intense pulses follow it), and negatively dispersed Temporal Airy Pulses (TAP-) with a TOD of -600.000 fs^3 (when at the beginning of the phase-modulated pulse there are sub pulses of low intensity, and the strongest pulse arrives last in the interaction zone).

2.2 Mechanical stress dicing

After laser writing on the surfaces, the quality of the ablated line was verified using a Differential Interference Contrast (DIC) reflection microscope to highlight the relief of the sample by increasing the image contrast. In this microscopy technique, the polarized light used to illuminate the specimen is split into two beams by a system of prisms mounted in the objective. When these two rays are reflected on different portions of the specimen, they will have different optical paths, and when the two

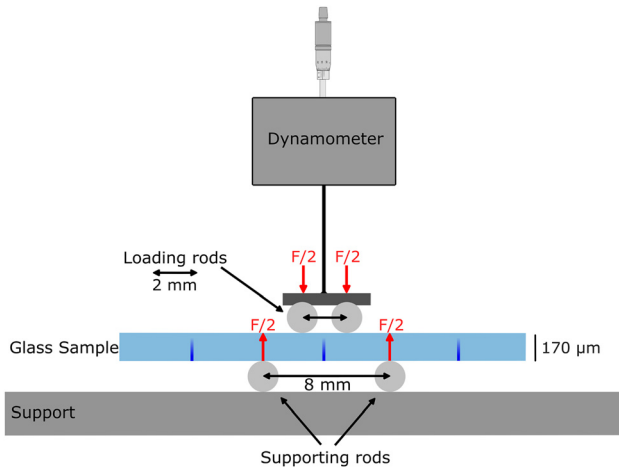


Figure 2: Scheme of in-house built four-point bending device.

rays recombine, interference figures will emphasize the corners and details. The samples were examined from top-view imaging, to measure the width of the scribed lines and to check the collateral ablation damage (see Figure 3A, for the $20\times$ objective, and Figure 7A, for the $50\times$ objective). The slides were then broken using an in-house built four-point bending device (design parameters are shown in Figure 2), and the breaking force was measured. The measurement of the breaking force was done manually by moving the micrometer screw on a Sauter dynamometer (50 N max force, 0.02 N resolution, 0.5 % accuracy) coupled to the upper rods. The dynamometer recorded the maximum force value (which occurs when the sample is broken) and this was used for further analysis. The samples were placed on the stress measuring device with the laser-scribed lines down, as indicated in the literature.²⁶ The parallel orientation of the written lines relative to the rods was maintained using a guide tool mounted along the long axis of the slides. A translation stage and a USB camera were used to position the scribed line exactly between the contact points of the two upper rods.

After breaking, the quality of the edges was again analyzed by DIC microscopy. Looking at the surface, from a top-view, defects that appeared along the break line, like chipping of the glass, were recorded, as represented in Figure 3B, for the $20\times$ objective and in Figure 7B, for the $50\times$ objective.

Additionally, looking from a side-view at the breaking walls of the glass sample, the quality of the laser cut groove and the neatness of the cross-section can be analyzed and compared for the three pulse shapes.

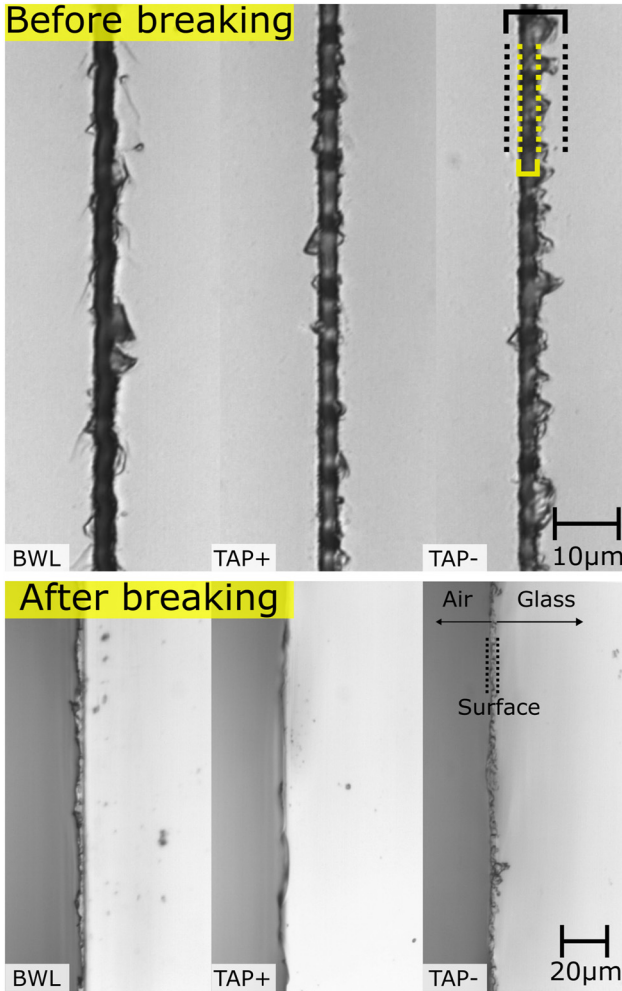


Figure 3: DIC microscopy images of the sample surface with laser ablation line performed with the 20 \times objective. (A) before breaking (magnified 100 \times), (B) after breaking (magnified 50 \times). Parameters: 1 μ J pulse energy, 0.5 mm/s scanning speed.

3 Results and discussion

Soda-lime glass has a very low optical absorption coefficient at 785 nm, which is why light at this wavelength can propagate far into the material. However, high absorption is present when focused ultrashort laser pulses with intensities exceeding the threshold for multiphoton ionization are used. In the literature, a band

gap value of 3.9 eV²⁷ is presented for soda-lime glass, which implies the simultaneous absorption of three photons²⁸ to generate quasi-free electrons in the conduction band as the first step in the laser-induced optical breakdown process. Even if impurities in the glass result in a smaller effective band gap value than that of pure fused silica, which requires six photons for multiphoton absorption,¹ Temporal Airy Pulses can still create high aspect ratio structures. To demonstrate the usability of TAP as a precursor in precision glass cutting, medium and tight focus conditions were investigated. In the following we present the results obtained using the two objectives (20× and 50×), both in terms of the quality of the ablation line (characterized by the width of the laser-written kerf and the smoothness of the breaking walls) and the force required to break the slides using these lines as a precursor.

3.1 Results obtained using the 20× medium power objective

High-resolution images of the laser-scribed line were taken from a top-view using a DIC microscope before (Figure 3A) and after (Figure 3B) dicing the samples. The images were analyzed using the software GIMP – GNU Image Manipulation Program (v.2.10.34) to align images and select areas of interest and Fiji: ImageJ (v.1.54f) to determine the ablated line width (with and without laser-induced collateral damage) of the written lines. In Figure 3A, the black dotted lines guide the eye to observe on the sample surface the area that includes the defects produced in the laser ablation process, and the yellow dotted lines represent the deep ablation area (kerf). The width of the kerf was measured as an average value in three representative areas (beginning, middle and end of the laser-written line) on the surface of the samples. For each temporal shape of the pulses, the minimum energy value represented is the one where the glass slides could still break, and not shatter.

The values are plotted as a function of ablation pulse energy in Figure 4, where each point represents the average values obtained for four scan lines produced under the same conditions on each glass slide and the error bars as standard deviation. It can be seen that lines written with TAP+ and TAP– are generally narrower and show fewer defects than lines written with BWL pulses. From the error bars shown in the plots of Figure 4, TAP+ also presents better reproducibility than the other pulse shapes, with a smaller standard deviation. They also produce a better edge quality after breaking the slides, as shown in Figure 3B, as it is straighter across the line with less splintering across the breaking wall.

Optical images of the breaking wall surface following dicing for the three temporal shapes (1 μJ pulse energy, 0.5 mm/s scanning speed) investigated as well as for the native side of the slide, separated with industrial methods, are shown in Figure 5. The depth of the laser ablation groove is indicated with yellow dashed lines.

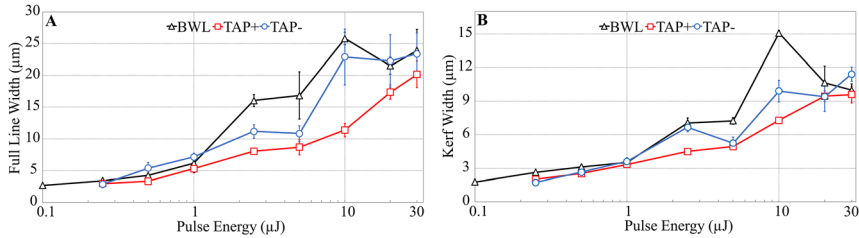


Figure 4: Measurement of laser-induced damage modifications using the 20× objective. Parameters: 0.1–30 µJ pulse energy, 0.5 mm/s scanning speed. (A) Averaged full line width, (B) Averaged kerf width, both as a function of pulse energy.

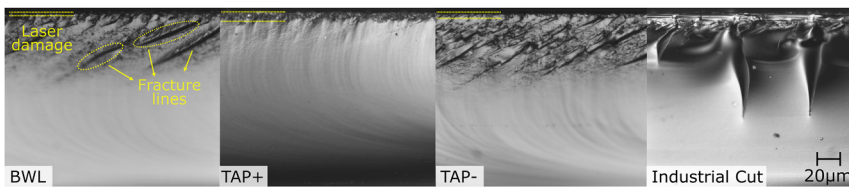


Figure 5: Surface roughness of cross-section samples after breaking; laser ablation line using the 20× objective. Parameters: 1 µJ pulse energy, 0.5 mm/s scanning speed.

The image shows that the kerf produced by TAP+ penetrates deeper inside the material, as it was also observed in the case of high-aspect-ratio structures produced in the single-shot regime.¹⁵ The quality of the post-break cross-section with these deeper grooves as a precursor is visibly better than when using BWL pulses and TAP−, where post-break defect lines and long cracks appear that propagate up to almost a third of the thickness of the glass slide.

To emphasize the high quality of our laser-based approach, Figure 5 (right) displays a cross-section of an industrial cut, which consist in using a diamond tip to scratch its surface and then breaking mechanically. It can be observed that the damage from the mechanical dicing process affected half of the section, with deep and uneven edge quality. Flatness and the absence of defects on the breakdown walls are an extremely important parameter in the quality of optoelectronic devices (e.g. LEDs and laser diodes) that are built on dielectric wafers as a substrate.²⁸

The breaking force of the glass slides on the ablation lines created by the three types of pulses is shown in Figure 6 for different scanning speeds, at a constant pulse energy of 30 µJ (A) and different pulse energies at a constant speed of 0.5 mm/s (B). At slow speeds, the laser pulses are more effective per position, inducing more damage, and resulting in a lower breaking force. The relative difference between pulse shapes is maintained across the speed interval. Since BWL pulses have a higher peak power

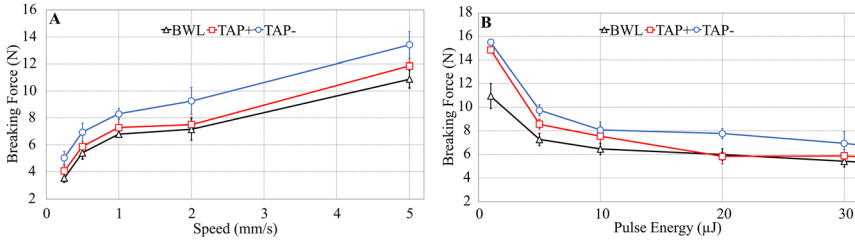


Figure 6: Breaking force using the 20× objective, (A) as a function of scanning speed (Parameters: 0.25–5 mm/s, 30 μJ constant pulse energy), and (B) as a function of pulse energy (Parameters: 1–30 μJ pulse energy, 0.5 mm/s constant scanning speed).

than Airy pulses,¹⁵ it is expected that at low energies or high travel speeds, they require the least force to break. However, for higher energies, the differences between BWL pulses and TAP+ become smaller because the latter is more effective in transferring laser energy to the dielectric sample, as TAP+ are not as affected as BWL pulses by the self-shielding effect and can create a free electron density above the ablation threshold over a greater depth within the material. The positively and negatively dispersed Temporal Airy Pulses create free electrons inside dielectric materials by addressing in a different way the two basic carriers' generation mechanisms, multiphoton and avalanche ionization. It has been numerically simulated¹ and experimentally measured^{16,17} that TAP+ produce a higher and longer distribution of the electronic density than the TAP- ones and this explains the difference between the breaking forces observed for the two cases.

3.2 Results obtained using the 50× high power objective

It is expected that when processing glass with high power microscope objectives, due to the better resolving power, the quality of the structures created on the surface will increase and thus, the grooves will have less thickness and fewer defects. Also, this type of objective favored the processing regime where high aspect ratio ablation structures were observed in single laser-pulse mode.¹⁵

DIC microscopy images of ablation grooves before and after glass slide breakage are presented in Figure 7. Compared to the medium power lens shown above, it can be observed (Figure 8) that the lines are thinner and with fewer defects before writing and smoother after breaking. Again, the ability of TAP+ to produce thinner and smoother ablation lines than BWL pulses over the entire range of energies investigated is highlighted.

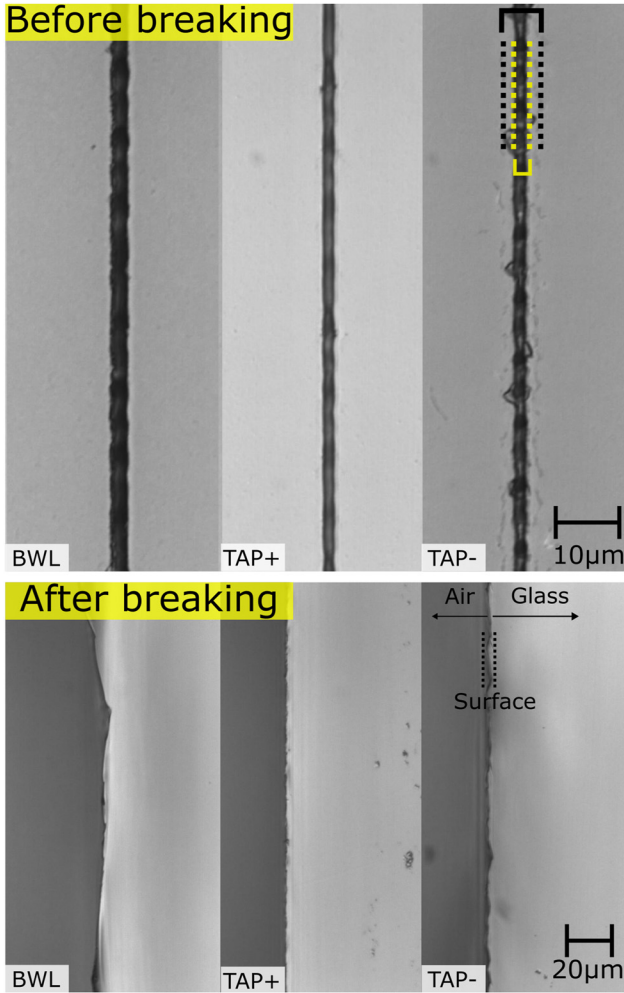


Figure 7: DIC microscopy images of the sample surface with laser ablation line performed with the 50 \times objective. (A) before breaking, (magnified 100 \times), (B) after breaking, (magnified 50 \times). Parameters: 0.5 μ J pulse energy, 0.5 mm/s scanning speed.

Images showing the break wall are represented in Figure 9 for the three pulse shapes and the original mechanically cut edge of the glass slide. For BWL pulses, the ablation kerf remains limited to shallow depths below the sample surface, while for TAP+, the grooves propagate deep inside the sample, over distances greater than 10 μ m. We consider this aspect an important advantage in the breaking process to obtain smooth walls without fragmentation defects, as it can be seen in Figure 9.

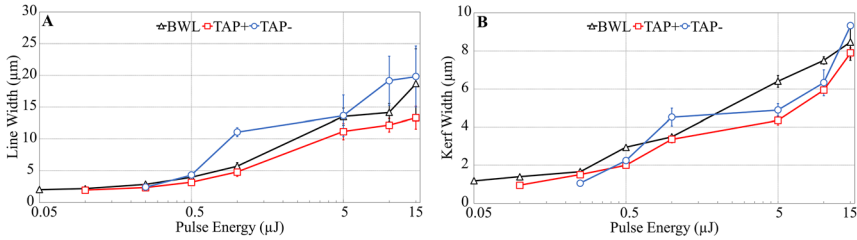


Figure 8: Measurement of laser-induced damage modifications using the 50 \times objective. Parameters: 0.1–15 μJ pulse energy, 0.5 mm/s scanning speed. (A) Averaged full line width, (B) Averaged kerf width, both as a function of pulse energy.

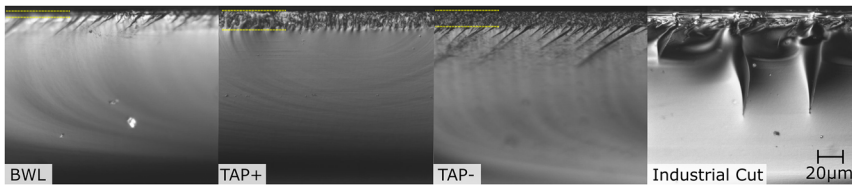


Figure 9: Surface roughness of cross-section samples; laser ablation line using 50 \times objective (0.5 μJ pulse energy, 0.5 mm/s scanning speed).

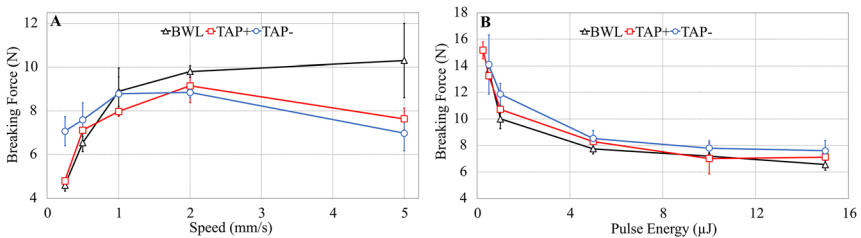


Figure 10: Breaking force using the 50 \times objective, (A) as a function of scanning speed (Parameters: 0.25–5 mm/s, 15 μJ constant pulse energy), and (B) as a function of pulse energy (Parameters: 1–15 μJ pulse energy, 0.5 mm/s constant scanning speed).

The effects of the high aspect ratio channels are noticeable in the breaking force graph as a function of speed (Figure 10A), individual laser damage spots (produced at the 1 kHz repetition rate of the laser) do not overlap at high speeds, allowing the creation of deeper channels, which is reflected in a lower required breaking force, while for BWL pulses the breaking force keeps increasing. All diced pieces had a good visible quality except for 5 mm/s speed for BWL pulses.

The breaking forces as a function of energy (Figure 10B) follow the theoretical expectations,¹⁵ where BWL pulses requires a lower amount of force due to its high

peak power, followed by TAP+ with deep high aspect ratio channels and TAP– requiring the highest force among those three.

With the decrease in energy, TAP+ stands out for achieving good visible quality diced pieces even at a pulse energy of 0.25 μJ . In contrast, BWL pulses and TAP– produced uneven diced pieces beginning at a pulse energy of 0.5 μJ . Even though the differences in breaking forces between the three forms of pulses are not very large, the quality of the fracture wall obtained with TAP+ is far superior to BWL pulses and traditional cutting methods. Since minor defects in the fracture walls can serve as crack and break points due to stress over time, we believe that this technique can improve the cutting quality of dielectric substrates and provides a valuable tool for researchers in materials science, microfabrication and related fields.

4 Conclusions

We have shown that temporally shaped femtosecond laser pulses in the form of Airy pulses, can be used to write grooves on the glass surface continuously with high lateral resolution and few collateral morphology defects. The ablation lines can be used as precursors in the mechanical cutting of soda-lime glass, with visibly better results than those obtained for femtosecond BWL pulses. We found that positive TAP produced a better overall cut quality. This effect is more pronounced when using tight-focusing conditions (50 \times objective) at high scanning speeds or low energies.

The advantage of TAP compared to Bessel beams or “Stealth” cutting, technologies used industrially in laser cutting, occurs at very low energies, when the TAP+ effect is increased, deeper channels are obtained, and wall quality images show this for thin glass samples. The proposed approach can potentially be used for neat and precise dicing of thin dielectric and semiconductor samples, where mechanical methods cannot produce acceptable results. It is predictable that for materials thinner than 170 μm with higher energy band gap, the positive effect towards dicing introduced by TAP will be more significant.

Acknowledgments: The authors wish to express their gratitude to Hendrike Braunknie and Arne Senftleben for the valuable discussions. The results were possible with the support of the Erasmus+ programme of the European Union and the partnership in POCU/993/6/13/153178, “Performanță în cercetare” - “Research performance” co-financed by the European Social Fund within the Sectorial Operational Program HumanCapital 2014-2020.

Research ethics: Not applicable.

Informed consent: Not applicable.

Author contributions: All authors have accepted responsibility for the entire content of this manuscript and approved its submission. M.S.R., C.S., and E.R.C. performed the measurements, analyzed data, and composed the manuscript. All authors participated in analytical discussions, and read and approved the manuscript.

Use of Large Language Models, AI and Machine Learning Tools: None declared.

Conflict of interest: The authors state no conflict of interest.

Research funding: None declared.

Data availability: Not applicable.

References

- Englert, L.; Rethfeld, B.; Haag, L.; Wollenhaupt, M.; Sarpe-Tudoran, C.; Baumert, T. Control of Ionization Processes in High Band Gap Materials via Tailored Femtosecond Pulses. *Opt. Express* **2007**, *15* (26), 17855–17862.
- Yadav, A.; Khashi, H.; Kolpakov, S.; Gordon, N.; Zhou, K.; Rafailov, E. U. Stealth Dicing of Sapphire Wafers with Near Infra-red Femtosecond Pulses. *Appl. Phys. A* **2017**, *123*, 369.
- Ogundairo, T. O.; Adegoke, D. D.; Akinwumi, I. I.; Olofinnade, O. M. Sustainable Use of Recycled Waste Glass as an Alternative Material for Building Construction – A Review. *IOP Conf. Mater. Sci. Eng.* **2019**, *640*, 012073.
- Karazi, S. M.; Ahad, I. U.; Benyounis, K. Y. Laser Micromachining for Transparent Materials. In *Reference Module In Materials Science and Materials Engineering*; Elsevier: Amsterdam, 2017.
- Nur-Luiza, R.; Che-Amat, R.; Ibrahim, M. N.; Shamshinar, S.; Syakirahafiza, M.; Mustaqqim, A. R. Utilization of Recycled Glass Waste as Partial Replacement of Fine Aggregate in Concrete Production. *Mater. Sci. Forum* **2014**, *803*, 16–20.
- Lei, W.; Kumar, A.; Yalamanchili, R. Die Singulation Technologies for Advanced Packaging: A Critical Review. *J. Vac. Sci. Technol. B: Microelectron. Nanometer Struct.* **2012**, *30* (4), 040801.
- Raj, M. M.; Cheong, K. Y.; Zainuriah, H. Ultrathin Wafer Pre-assembly and Assembly Process Technologies: A Review. *Crit. Rev. Solid State Mater. Sci.* **2015**, *40*, 1–40.
- Choi, J.; Kim, R.; Song, D.; Cho, D. W.; Suh, J.; Kim, S.; Ahn, S. H. Analysis of Laser Cutting Process for Different Diagonal Material Shapes. *Processes* **2022**, *10* (12), 2743.
- Lum, K. C. P.; Ng, S. L.; Black, I. CO2 Laser Cutting of MDF: 1. Determination of Process Parameter Settings. *Opt Laser. Technol.* **1999**, *32*, 67–76.
- Lian, M.; Seo, Y.; Lee, D. An Experimental Investigation on the Cutting Quality of Three Different Rock Specimens Using High Power Multimode Fiber Laser. *Materials* **2021**, *14* (11), 2972.
- Arshed, F.; Ahmad, A.; Xirouchakis, P.; Metsios, I. Laser Cutting of Carbon Fiber Reinforced Plastic Components for Remanufacturing. *J. Remanufacturing* **2022**, *12*, 411–433.
- Du, X.; Camilo, F.; Craig, B. A. Multi-focal Laser Processing in Transparent Materials Using an Ultrafast Tunable Acoustic Lens. *Opt. Lett.* **2022**, *47*, 1634–1637.
- Dudutis, J.; Stonys, R.; Račiukaitis, G.; Gečys, P.; Hellmann, R.; Račiukaitis, G.; Gečys, P. Glass Dicing with Elliptical Bessel Beam. *Procedia CIRP* **2019**, *94*, 957–961.
- Englert, L.; Wollenhaupt, M.; Sarpe, C.; Otto, D.; Baumert, T. Morphology of Nanoscale Structures on Fused Silica Surfaces from Interaction with Temporally Tailored Femtosecond Pulses. *J. Laser Appl.* **2012**, *24*, 5, 042002.

15. Götte, N.; Winkler, T.; Meinl, T.; Kusserow, T.; Zielinski, B.; Sarpe, C.; Senftleben, A.; Hillmer, H.; Baumert, T. Temporal Airy Pulses for Controlled High Aspect Ratio Nanomachining of Dielectrics. *Optica* **2016**, *3*, 389–395.
16. Sarpe, C.; Köhler, J.; Winkler, T.; Wollenhaupt, M.; Baumert, T. Real Time Observation of Transient Electron Density in Water Irradiated with Tailored Femtosecond Laser Pulses. *New J. Phys.* **2012**, *14*, 16, 075021.
17. Winkler, T.; Sarpe, C.; Jelzow, N.; Lillevang, L. H.; Götte, N.; Zielinski, B.; Balling, P.; Senftleben, A.; Baumert, T. Probing Spatial Properties of Electronic Excitation in Water after Interaction with Temporally Shaped Femtosecond Laser Pulses: Experiments and Simulations. *Appl. Surf. Sci.* **2016**, *374*, 235–242.
18. Salman, N.; Lin, L.; Sheikh, M. A. Laser Glass Cutting Techniques - A Review. *JLA Celebrates 60th Anniv. Laser* **2013**, *25* (4), 11.
19. Shuting, L.; Xin, Z.; Xiaoming, Y. H.; Anming, V.; Sinisa, J.; Martin, J.; Hang-Eun, Y.; Yung, C. S.; Shin, Y. C. Ultrafast Laser Applications in Manufacturing Processes: A State of the Art Review. *J. Manuf. Sci. Eng.* **2020**, *142*, 1–43.
20. Neugebauer, J. Determination of Bending Tensile Strength of Thin Glass. *Gent. Challenging Glass* **2016**, *5*. <https://doi.org/10.7480/cgc.5.2267>.
21. Präckelt, A.; Wollenhaupt, M.; Assion, A.; Horn, C.; Sarpe-Tudoran, C.; Winter, M.; Baumert, T. Compact, Robust and Flexible Setup for Femtosecond Pulse Shaping. *Rev. Sci. Instrum.* **2003**, *73*, 4950–4953.
22. Xu, Z.; Yao, L.; Haibo; Qiang, W.; Xitan, X.; Lu, C.; Zhixuan, Li; Rui, W.; Jin, G.; Jingjun, X.; Köhler, J.; Wollenhaupt, M.; Bayer, T.; Sarpe, C.; Baumert, T. Zeptosecond Precision Pulse Shaping. *Opt. Express* **2011**, *19*, 11638–11653.
23. Wu, Q.; Zhou, X.; Lu, Y.; Liu, H.; Xu, X.; Chen, L.; Li, Z.; Wang, R.; Guo, J; Xu, J One-step Crack-free Fabrication of Chip-Scale Lithium Niobate through Dispersion Engineering of Femtosecond Pulses. *Optica Open* **2023**, *13*. <https://doi.org/10.1364/opticaopen.22068122.v1>.
24. Englert, L.; Wollenhaupt, M.; Haag, L.; Sarpe-Tudoran, C.; Rethfeld, B.; Baumert, T. Material Processing of Dielectrics with Temporally Asymmetric Shaped Femtosecond Laser Pulses on the Nanometer Scale. *Appl. Phys. A* **2008**, *92*, 749–753.
25. Down-drawn Sheet Dimensions the Following Specifications Are Relevant for D 263® T Eco, D 263® LA Eco, and AS 87 Eco. [Online] Schott. <https://www.schott.com/en-ae/products/sheets-p1000333/technical-details?tab=edd72300813544dc901a84bc390fb7c9> (Accessed 2024-05-20).
26. Domke, M.; Egle, B.; Stroj, S.; Bodea, M.; Schwarz, E.; Fasching, G. Ultrafast-laser Dicing of Thin Silicon Wafers: Strategies to Improve Front- and Backside Breaking Strength. *Appl. Phys. A* **2017**, *123*, 746.
27. Gräf, S.; Kunz, C.; Müller, F. A. Formation and Properties of Laser-Induced Periodic Surface Structures on Different Glasses. *Materials* **2017**, *10*, 933.
28. Shehataa, A.; Ali, M.; Schuchb, R.; Mohameda, T. Experimental Investigations of Nonlinear Optical Properties of Soda-Lime Glasses and Theoretical Study of Self-Compression of Fs Laser Pulses. *Opt. Laser Technol.* **2019**, *116*, 276–283.